Power Quality Improvement in Grid-Connected PV Systems Using Sequence Control

Priyank Nema[1†] and **V Sivasankaran**[2], Non-members

ABSTRACT

A modified control strategy for grid-connected inverters is presented to enhance the integration of renewable energy sources while effectively addressing challenges arising from unhealthy voltage and current conditions. The study introduces an improved instantaneous reactive power theory–based control scheme that utilizes positive-sequence components of grid voltages and negative-sequence components of load currents to regulate the grid-tied converter. To further enhance dynamic performance, a proportional–integral controller is incorporated to maintain dc-link voltage stability under abnormal grid and load scenarios. The proposed control approach is implemented and validated in MATLAB/Simulink across a range of operating conditions, including steady-state, dc offset, grid harmonics, unbalanced grid voltages, and non-linear as well as unbalanced loads, both with and without solar PV integration. Simulation results demonstrate significant improvements in power factor correction and reactive power compensation, with robust controller performance under varying irradiance levels. Comparative analysis with recent control schemes highlights the superior performance and effectiveness of the proposed method. Moreover, the total harmonic distortion values obtained across multiple test cases comply with IEEE-519 standards, confirming the reliability and robustness of the proposed control technique for grid-connected renewable energy systems.

Keywords: Positive and negative sequence component, VSI, Solar PV, Power quality, Unhealthy grid, IIRPT

1. INTRODUCTION

The growing electricity demand resulting from rapid industrialization and rural electrification has intensified the need for integrating renewable energy sources alongside conventional non-renewable resources to meet increasing load requirements. Renewable energy technologies not only alleviate the depletion of conventional energy reserves but also mitigate environmental impacts, minimize power losses, reduce operational costs, and improve voltage profiles, thus contributing to the development of sustainable and resilient power systems. According to projections, the share of renewable energy in distribution networks is expected to increase significantly, from 14% to 63% by 2050 [1]. This integration, commonly referred to as Distributed Generation (DG), however, introduces several Power Quality (PQ) issues—including voltage fluctuations, reactive power imbalances, harmonic distortion, and excessive neutral current—that can adversely affect grid stability and overall power reliability. Among various renewable technologies, photovoltaic (PV) systems have emerged as the most rapidly expanding source of clean energy across both residential and commercial sectors, driven by technological advancements and supportive government policies [2]. Despite their numerous advantages, photovoltaic (PV) systems encounter challenges associated with efficiency, grid stability, and power quality (PQ). Harmonic distortions in PV systems primarily originate from power electronic interfaces, non-linear loads (NLL) connected at the Point of Common Coupling (PCC), and contaminated grid conditions prevalent in regions such as India. These factors contribute to unbalanced voltages, dc offsets, and various other PQ disturbances. Addressing these issues is essential to ensure compliance with IEEE Std. 519-2014, which specifies permissible harmonic distortion limits based on system voltage levels [3]. The inverter connected to a Distributed Generation (DG) system can effectively function as a PQ conditioner, thereby enhancing overall system performance.

To maximize the energy extraction from solar photovoltaic (PV) panels, various Maximum Power Point Tracking (MPPT) techniques—such as Perturb and Observe (P&O) [4], Incremental Conductance [5], and artificial intelligence-based algorithms—are employed. These techniques generate switching signals that control the Insulated-Gate Bipolar Transistors (IGBTs) within DC–DC converters, ensuring efficient impedance matching and optimal energy transfer. Voltage Source Inverters (VSIs) play a critical role in grid integration, operating as active power filters or Distribution STATic COMpensators (DSTATCOMs) to mitigate PQ issues [6]. By injecting compensating anti-harmonic currents, DSTATCOMs enhance grid performance and stability. A wide range of control algorithms—from conventional schemes to adap-

Manuscript received on October 6, 2025; revised on December 30, 2025; accepted on January 5, 2026. This paper was recommended by Associate Editor Chawasak Rakpenthai.

[1]The author is with Department of Computer Science & Engineering, Lakshmi Narain College of Technology & Science, Bhopal, Kalchuri Nagar, Raisen Road, Bhopal - 462022, Madhya Pradesh, India.

[2]The author is with School of Electrical and Electronics Engineering, VIT Bhopal University, Sehore, Bhopal-Indore Highway, Kothrikalan, Sehore, Madhya Pradesh - 466114, India.

[†]Corresponding author: priyankn@lnct.ac.in

Digital Object Identifier: 10.37936/ecti-eec.2026241.258738

tive and generalized integrator-based approaches—have been developed to effectively address PQ disturbances in DG-connected systems. Conventional control algorithms used to mitigate power quality issues in grid-connected solar PV systems include Synchronous Reference Frame (SRF) theory-based controllers [7], Instantaneous Reactive Power Theory (IRPT) controllers [8], sliding mode controllers, Kalman filter techniques, wavelet-transform methods, and Discrete Fourier Transform (DFT) approaches. While these methods are widely adopted due to their simplicity and ease of implementation, they exhibit several drawbacks. SRF and IRPT controllers often fail to perform adequately under grid voltage disturbances, leading to slow dynamic responses and ineffective compensation for harmonics and unbalanced loads.

Sliding mode controllers, though robust, introduce chattering effects that degrade system stability. Kalman filter techniques are computationally intensive and sensitive to modelling inaccuracies, while wavelet-transform and DFT methods struggle with real-time adaptability, limiting their ability to address sudden grid fluctuations and DC offsets. To overcome these limitations, adaptive control algorithms have been developed, including ADALINE (ADAptive LInear NEuron) [9], Recursive Least Square (RLS) [10], Least Mean Square (LMS) [11], Least Mean Fourth (LMF) [12], Improved Linear Sinusoidal Tracer (ILST) [13], Variable Step Size Least Mean Square (VSSLMS) [14], and Adaptive Notch Filter (ANF) [15]. These adaptive controllers provide better tracking and compensation under varying load conditions. However, they also possess significant disadvantages. Adaptive controllers are computationally complex, requiring extensive tuning and longer processing times, which can hinder real-time performance.

Additionally, they often fail to eliminate the effects of DC offsets in grid voltages, grid harmonics, and unbalanced grid conditions, which are critical for ensuring stable power quality. To address the shortcomings of adaptive controllers, generalized integrator-based control algorithms such as second-Order Generalized Integrator (SOGI) [16], Improved SOGI (ISOGI) [17], Mixed Second and Third OGI (MSTOGI) [18], Cascaded SOGI (CSOGI) [19], Second-Order SOGI (SOSOGI) [20], Cascaded Non- Identical SOGI (CNISOGI) [21], Fifth OGI (FOGI) [22] and Sixth OGI (SiOGI) [23] have been introduced. These methods enhance harmonic extraction and improve dynamic response. Despite their advantages, generalized integrator controllers are complex to implement and require careful design to prevent stability issues, particularly under rapidly fluctuating grid conditions. Conventional controllers, while easy to implement, lack the capability to operate effectively under unhealthy grid voltage conditions and exhibit slow response times. In contrast, adaptive and generalized integrator controllers, though more effective, are complex and challenging to deploy in practical applications.

To overcome these limitations, this research introduces an improved IRPT (IIRPT) control scheme that incorporates positive and negative sequence component extraction. The proposed IIRPT first calculates the positive sequence component from unhealthy grid voltages, addressing power quality issues introduced by grid disturbances. Simultaneously, it calculates the negative sequence component from load currents, compensating for harmonic distortions. By integrating these two blocks into the conventional IRPT framework, the system achieves faster response times and enhanced capability to manage unhealthy grid conditions, ensuring robust and reliable grid-connected solar PV performance.

The paper is structured as follows. Section I provides an introduction to the research topic. Section II describes the modelling of the grid-connected solar photovoltaic (PV) system. Section III discusses the conventional control scheme, while Section IV details the proposed control approach. Section V presents the simulation results and corresponding analyses, followed by a comparative evaluation of the proposed method in Section VI. Finally, Section VII concludes the paper by summarizing the key findings and highlighting potential directions for future work.

2. MODEL DESCRIPTION OF THE GRID-CONNECTED SOLAR PV SYSTEM

Figure 1 shows the proposed system model. The proposed system model addresses power quality issues in a grid-connected solar photovoltaic (PV) system through an advanced integration of power electronics and control strategies. The system connects a three-phase grid to the solar PV array via a Voltage Source Inverter (VSI) and a DC-DC boost converter. To ensure maximum power extraction from the solar PV, Maximum Power Point Tracking (MPPT) is implemented using the Perturb and Observe (P&O) algorithm. The MPPT algorithm generates a control signal for the DC-DC boost converter to achieve impedance matching, ensuring that maximum power is delivered to the load, with any surplus directed to the grid. The output of the DC-DC converter is connected to the VSI, which functions as a shunt active power filter. A Proportional-Integral (PI) controller is employed to maintain a constant voltage across the DC link capacitor, ensuring stable operation of the VSI. Interfacing inductors are incorporated between the solar PV and the grid to minimize current ripple. The system also addresses harmonic distortions generated by a nonlinear and unbalanced load through the use of an IIRPT-based controller. This controller generates a compensation signal, which is processed by a hysteresis controller to produce anti-harmonic currents for effective mitigation. Furthermore, the proposed model accommodates an unhealthy grid with line impedance, enhancing its applicability to practical scenarios. This integrated approach effectively mitigates power quality issues, ensuring efficient and reliable operation of the grid-connected solar PV system. All the simulation parameter values utilized in this study are presented in

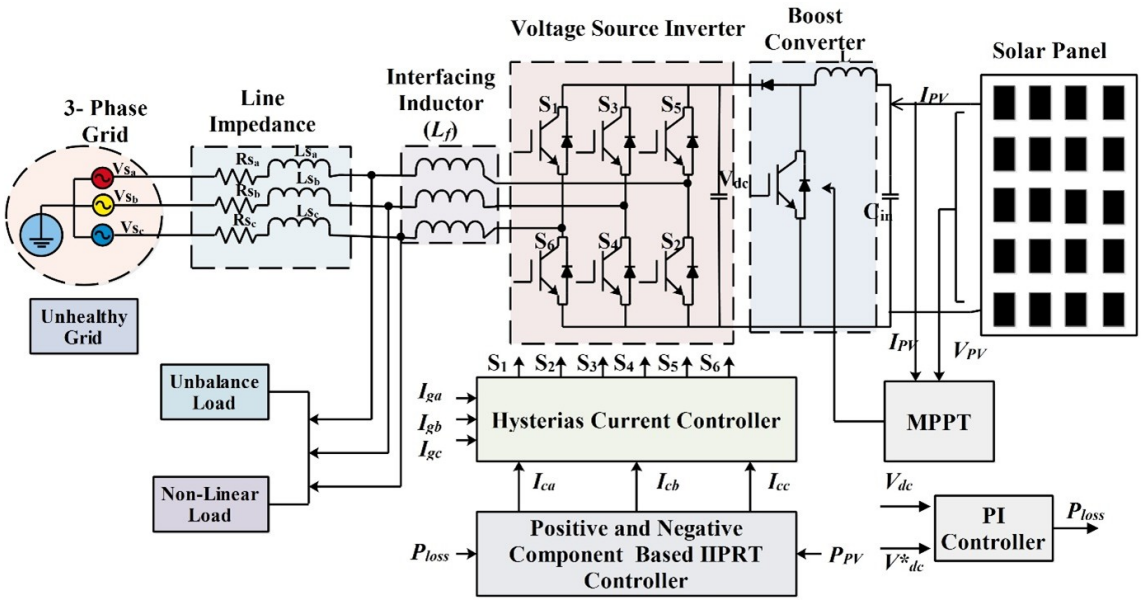

***Fig. 1**: Proposed system mode.*

***Table 1**: Design parameters of PV cell, boost converter, DC link capacitor, interfacing inductor, PI controller gain.*

Specification	Silmulation Value
PV Power	33.5 kW
Irradiation (G)	1,000 W/m^2
Open circuit voltage (V_{oc})	36.6 V
Short circuit current (I_{sc})	7.97 A
Maximum power point voltage (V_{mp})	29.3 V
Maximum power point current (I_{mp})	7.47 A
Series panels	17
Parallel panels	9
Line inductance (L)	4.5 mH
Three phase grid voltage (V_g)	415 V
Supply frequency (f)	50 Hz
DC link voltage (V_{dc})	700 V
Interfacing inductor (L_f)	3 mH
DC link capacitor (C_{dc})	4,500 μF
Line impedance (Z_1)	$R = 0.01\Omega$ $L = 0.72$ mH
Proportional gain (K_P)	2
Integral gain (K_I)	0.1

Table 1.

3. CONVENTIONAL IRPT

Figure 2 represent the block diagram of the Instantaneous Reactive Power Theory (IRPT) based controller, also known as the p–q theory, is a powerful and widely used control algorithm for mitigating power quality issues in grid-connected solar photovoltaic (PV) systems. This algorithm is based on the instantaneous analysis

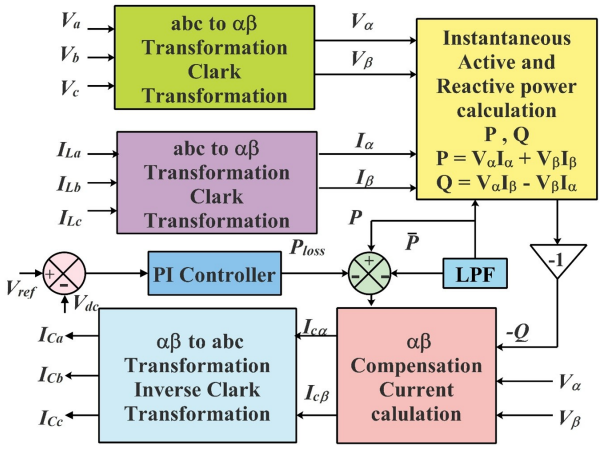

***Fig. 2**: Conventional instantaneous reactive power controller.*

of three-phase currents and voltages in the stationary $\alpha\beta$ coordinate system, obtained through Clarke transformation. The IRPT decomposes the load currents into instantaneous active ($\boldsymbol{P}$) and reactive ($\boldsymbol{Q}$) power components, enabling the identification and extraction of unwanted components such as harmonics, unbalanced currents, and reactive power in real time. The reference compensating currents are derived by eliminating the oscillatory and reactive parts of the instantaneous power, leaving only the fundamental active power component that should be supplied by the grid. These reference currents are then converted back to the three-phase system and tracked by the inverter using a current control strategy, typically implemented with hysteresis or PWM-based modulation techniques. By dynamically injecting these compensating currents into the grid, the IRPT-based control algorithm effectively suppresses

harmonics, balances unbalanced loads, and provides reactive power support, thereby enhancing the overall power quality, improving voltage stability, and ensuring efficient integration of solar PV systems with the utility grid. However, the conventional IRPT-based controller is unable to effectively handle unhealthy grid voltage conditions, such as DC offsets, harmonics, and unbalanced grid voltages. To enhance its adaptability and overcome these limitations, improvements are required in the control strategy. In this research, an Improved IRPT (IIRPT)-based controller is proposed, where, instead of directly utilizing the ($\alpha\beta$) components of the grid voltage, the positive-sequence component of the grid voltage is employed. Similarly, in place of the ($\alpha\beta$) components of the load current, the negative-sequence component of the load current is used. This modification enhances the capability of the controller, enabling it to effectively address unhealthy grid voltage conditions and thereby improving overall system performance.

4. PROPOSED CONTROL ALGORITHM

The proposed controller algorithm is systematically organized into three subsections to ensure a comprehensive approach to achieving effective control. The first subsection details the methodology for calculating the positive and negative sequence components of the grid voltage and load current, which are crucial for accurately capturing the asymmetries and imbalances in the system. Building on this, the second subsection elaborates on the generation of the reference signal using these extracted sequence components, ensuring that the control objectives align with the desired operational conditions. Finally, the third subsection outlines the process of generating the firing signals through a hysteresis controller, which provides precise switching actions to achieve robust and stable performance. Together, these subsections integrate seamlessly to form a cohesive and efficient controller design.

4.1 Extraction of positive and negative sequence component stage

In electrical engineering, the positive and negative sequence components are critical for analysing three-phase systems under various unhealthy conditions. The positive sequence component represents a balanced set of three-phase phasors rotating in the same direction as the original system, whereas the negative sequence component represents a set of phasors rotating in the opposite direction. These phasors may exhibit balanced or unbalanced magnitudes and phase differences. In this study, the positive sequence component of an unhealthy three-phase grid voltage is determined using symmetrical component theory, providing a balanced representation of the grid voltage. Meanwhile, the negative sequence component is derived from the three-phase nonlinear and unbalanced load current using the same theory. The negative sequence component of the load current highlights system unbalances, which can lead to harmonics, overheating, or equipment damage. The positive sequence voltage (V_1) is calculated from the grid voltages (V_{ga}, V_{gb}, V_{gc}) using the following equation.

$$\begin{cases} V_{a1} = \frac{1}{3}\left(V_{ga} + \lambda V_{gb} + \lambda^2 V_{gc}\right) \\ V_{b1} = \lambda^2\left(V_{a1}\right) \\ V_{c1} = \lambda(V_{a1}) \end{cases} \tag{1}$$

and the negative sequence current (I_2) is computed from the load currents (I_{La}, I_{Lb}, I_{Lc}) using following equations.

$$\begin{cases} I_{a2} = \frac{1}{3}\left(I_{La} + \lambda^2 I_{Lb} + \lambda I_{Lc}\right) \\ I_{b2} = \lambda^2\left(I_{a2}\right) \\ I_{c2} = \lambda(I_{a2}) \end{cases} \tag{2}$$

where ($e^{j2\pi/3}$) denotes the 120° phase shift operator. This approach is fundamental for the precise analysis, mitigation of system imbalances, and effective control of three-phase systems in modern power grids.

4.2 Improved instantaneous reactive power theory

Figure 3 shows the modified Instantaneous Reactive Power Technique is a modified form of Instantaneous Reactive Power Theory. The modified Instantaneous Reactive Power Technique uses the positive sequence component of grid voltage and the negative sequence component of load current to obtain the reference voltage. Firstly, the value of positive sequence component V_{a1}, V_{b1}, V_{c1} of V_{gabc} which is grid voltage is obtained, and the value of negative sequence component I_{a2}, I_{b2}, I_{c2} of load current I_{Labc} is obtained. After that, with the help of Clark's transformation of positive sequence voltage and negative sequence current, the value of $\alpha\beta$ component has been obtained through the following equation.

$$\begin{bmatrix} V_{\alpha1} \\ V_{\beta1} \end{bmatrix} = \sqrt{2/3} \begin{bmatrix} 1 & -1/\sqrt{2} & -1/\sqrt{2} \\ 0 & \sqrt{3}/2 & -\sqrt{3}/2 \end{bmatrix} \begin{bmatrix} V_{a1} \\ V_{b1} \\ V_{c1} \end{bmatrix} \tag{3}$$

$$\begin{bmatrix} I_{\alpha2} \\ I_{\beta2} \end{bmatrix} = \sqrt{2/3} \begin{bmatrix} 1 & -1/\sqrt{2} & -1/\sqrt{2} \\ 0 & \sqrt{3}/2 & -\sqrt{3}/2 \end{bmatrix} \begin{bmatrix} I_{a2} \\ I_{b2} \\ I_{c2} \end{bmatrix} \tag{4}$$

where V_{a1}, V_{b1}, V_{c1} represents the positive sequence component of the grid voltage and I_{a2}, I_{b2}, I_{c2} represents the negative sequence component of the load current $V_{\alpha1}$, $V_{\beta1}$ represent the positive sequence voltage of $\alpha\beta$ and $I_{\alpha2}$, $I_{\beta2}$ represent the negative sequence current of $\alpha\beta$ current.

After that with the help of $V_{\alpha1}$, $V_{\beta1}$, $I_{\alpha2}$ and $I_{\beta2}$ the value of active and reactive power can be determined with the help of the following equations.

$$\begin{bmatrix} P \\ Q \end{bmatrix} = \begin{bmatrix} I_{\alpha2} & I_{\beta2} \\ -I_{\beta2} & I_{\alpha2} \end{bmatrix} \begin{bmatrix} V_{\alpha1} \\ V_{\beta1} \end{bmatrix} \tag{5}$$

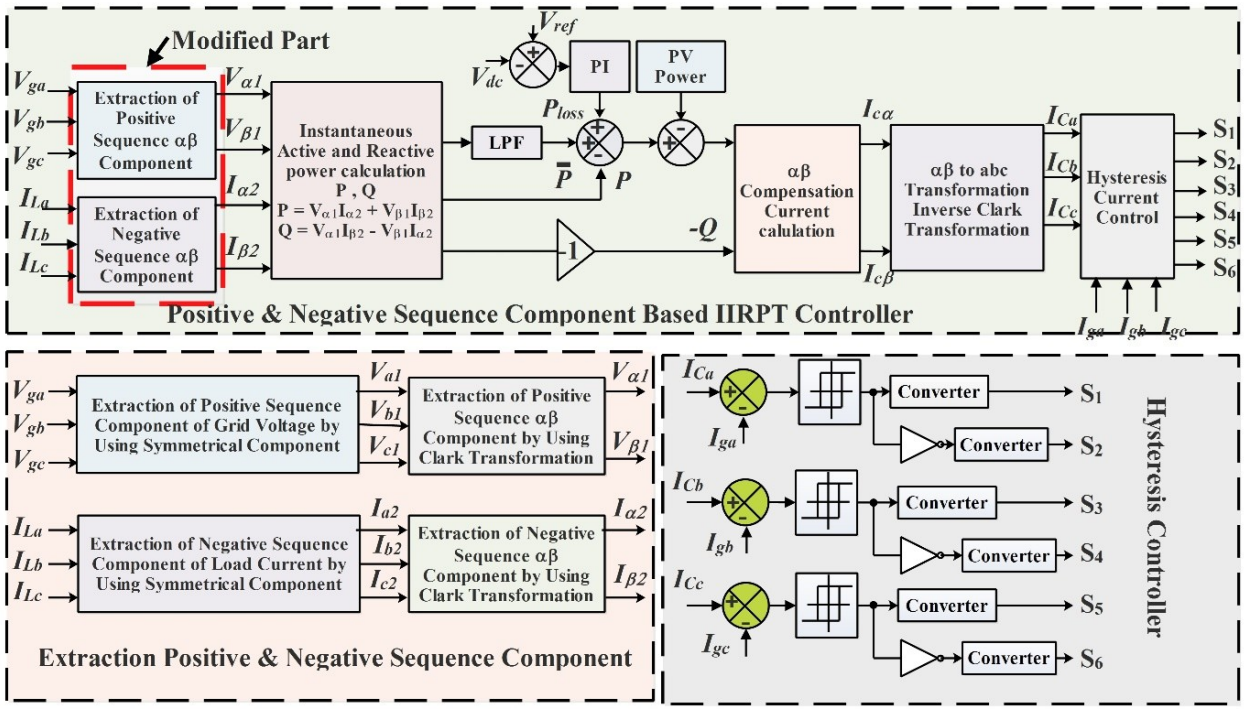

***Fig. 3**: Positive and negative sequence component based IIRPT controller.*

After calculating the active and reactive power, the AC component of the active power and the full reactive power are utilized to generate the ($\alpha\beta$) components of the compensation current. The active power contains both AC and DC components. To extract the AC component, the DC component of the active power is first subtracted from the total active power. The DC active power is obtained using a low-pass filter (LPF). After determining the AC component, the power loss component (P_{loss}) is added, and the photovoltaic (PV) output power is subtracted. The addition of (P_{loss}) accounts for the switching losses of the voltage source inverter (VSI), which also generates harmonics, necessitating harmonics compensation in the current. The subtraction of PV-generated power ensures the proper balance of power flow between the grid and the load. This balance maintains a steady power supply from the grid to the load when solar irradiance is 0 W/m^2 and ensures the residual power flows back to the grid when solar irradiance is 1000 W/m^2. The AC active power is calculated using the equation provided below.

$$P_{ac} = P - P_{dc} + P_{loss} - P_{PV} \tag{6}$$

The value of $\alpha\beta$ reference voltage can be determined with the help of the following equations.

$$\begin{bmatrix} I_{c\alpha} \\ I_{c\beta} \end{bmatrix} = \frac{1}{V_{\alpha1}^2 + V_{\beta1}^2} \begin{bmatrix} V_{\alpha1} & -V_{\beta1} \\ V_{\beta1} & V_{\alpha1} \end{bmatrix} \begin{bmatrix} P_{ac} \\ -Q \end{bmatrix} \tag{7}$$

With the help of inverse Clark transformation to $\alpha\beta$ reference voltage, the value of *abc* reference voltage can be determined with the help of the following equations.

$$\begin{bmatrix} I_{ca} \\ I_{cb} \\ I_{cc} \end{bmatrix} = \sqrt{2/3} \begin{bmatrix} 1 & 1 \\ -1/2 & \sqrt{3}/2 \\ -1/2 & -\sqrt{3}/2 \end{bmatrix} \begin{bmatrix} I_{c\alpha} \\ I_{c\beta} \end{bmatrix} \tag{8}$$

The switching signal for the voltage source inverter is generated using the hysteresis voltage controller.

4.3 Calculation of firing signal for the VSI

After calculating the reference signal, a hysteresis controller is employed to generate the firing signals for the Voltage Source Inverter (VSI). The hysteresis controller operates by comparing the generated reference signal with the grid current, both of which serve as its inputs. This comparison determines whether the VSI should switch its state to produce the required anti-harmonic current. The controller maintains the output current within a predefined hysteresis band around the reference signal. Whenever the current deviates beyond the upper or lower bounds of this band, the hysteresis controller adjusts the VSI switching state accordingly, ensuring accurate tracking of the reference signal. This dynamic switching effectively minimizes harmonic distortions and enhances the overall power quality.

5. RESULTS AND DISCUSSION

5.1 Simulation results under various grid voltage condition with solar irradiance 1000 W/m^2

Figures 4, 5, 6, and 7 present the simulation results under various grid voltage scenarios with both nonlinear

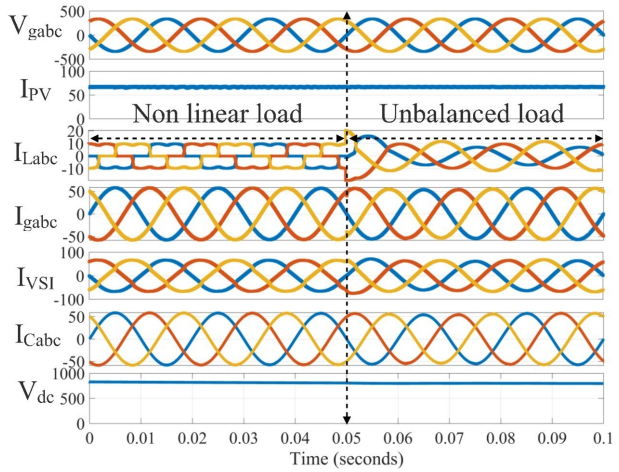

***Fig. 4**: Simulation under healthy grid voltage with non-linear and unbalanced load condition at a solar irradiance of 1000 W/m^2.*

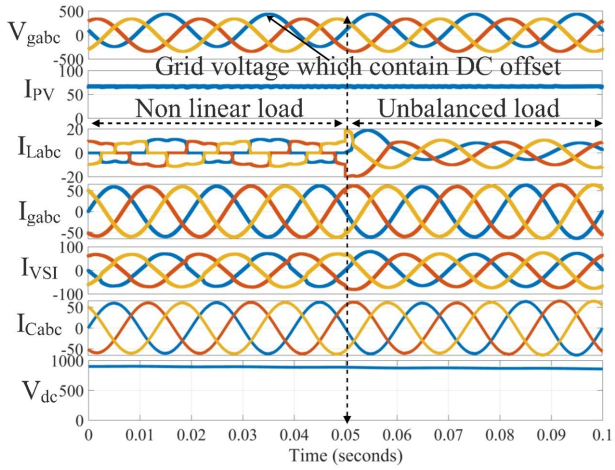

***Fig. 5**: imulation under grid voltage with DC offset, non-linear and unbalanced load condition at a solar irradiance of 1000 W/m^2.*

and unbalanced load conditions, considering a constant solar irradiance of 1000 W/m². Under these conditions, power flows from the solar PV system to the load, with any excess power being supplied to the grid. Specifically, Figure 4 depicts the simulation results under a healthy grid voltage condition, Figure 5 illustrates the scenario with a DC offset in the grid voltage, Figure 6 represents the grid voltage with harmonics, and Figure 7 demonstrates the unbalanced grid voltage condition. Each of these simulations includes seven distinct waveforms: three-phase grid voltage, solar PV-generated current, three-phase load current, three-phase grid current, voltage source inverter output current, compensation current, and DC link voltage. In all cases, a non-linear load is connected for half of the simulation time, while an unbalanced load is connected for the remaining half. In Figure 5 a DC voltage source is used to introduce the DC offset component, while, in Figure 6, a three-phase programmable voltage source block in MATLAB Simulink is utilized to introduce harmonics. Similarly, in Figure 7, an unbalanced grid voltage is generated using a three-phase voltage source in which the phase magnitudes are varied. Prior to the application of the controller, the grid current is significantly distorted and non-sinusoidal; however, after implementing the controller, the grid current is effectively regulated to a purely sinusoidal waveform. The FFT analysis of the grid current, as shown in Table 2, confirms that the total harmonic distortion (THD) is reduced to below 5%, demonstrating the effectiveness of the proposed control strategy in improving power quality in grid-tied solar PV systems.

5.2 Simulation results under various grid voltage scenario with solar irradiance 0 W/m^2

Figures 8, 9, 11, and 12 illustrate the simulation results under various grid voltage conditions, considering a nonlinear and unbalanced load with solar irradiance at

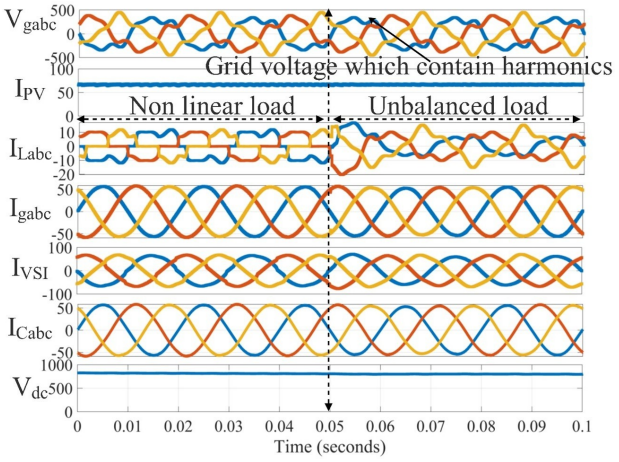

***Fig. 6**: Simulation under grid voltage with harmonics, non-linear and unbalanced load condition at a solar irradiance of 1000 W/m^2.*

0 W/m². This scenario implies that the solar PV system does not generate electricity and, as a result, the power flows entirely from the grid to the load. Specifically, Figure 8 represents the simulation results under a healthy grid voltage condition, while Figure 9 shows the scenario where the grid voltage contains a DC offset. Figure 10 presents the case of harmonic grid voltage, and Figure 11 illustrates the simulation results under an unbalanced grid voltage condition. Each of these figures contains six waveform representations, which include the three-phase grid voltage, three-phase load current, three-phase grid current, three-phase voltage source inverter (VSI) output current, compensation current, and DC-link voltage. The analysis of these simulation results reveals that before the implementation of the controller, the grid current is not completely sinusoidal and contains significant harmonic distortions. However, after applying the controller, the grid current becomes nearly sinusoidal, as confirmed by the Fast Fourier Transform (FFT) analysis

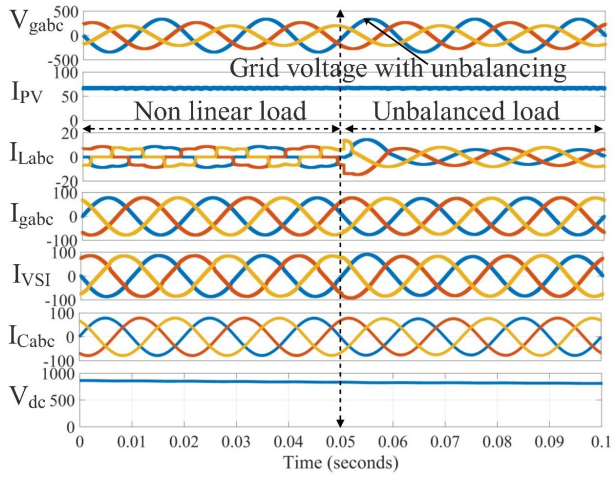

***Fig. 7**: Simulation under unbalanced grid voltage conditions with nonlinear and unbalanced loads at a solar irradiance of 1000 W/m^2.*

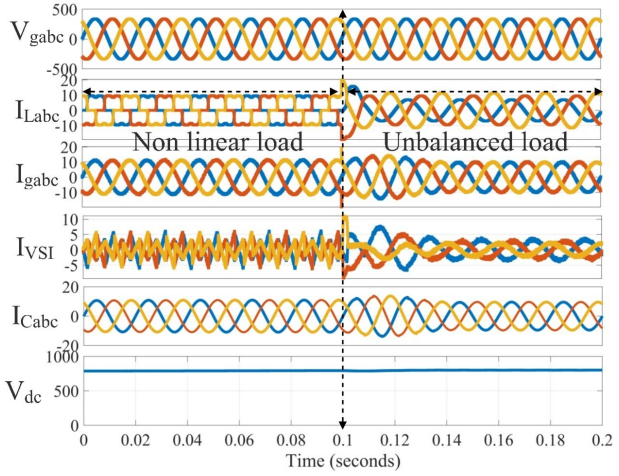

***Fig. 8**: Simulation under healthy grid voltage with nonlinear and unbalanced load condition at a solar irradiance of 0 W/m^2.*

shown in Table 2. The FFT analysis demonstrates that under all the considered grid voltage scenarios and different load conditions, the Total Harmonic Distortion (THD) in the grid current remains below 5%, ensuring compliance with standard power quality requirements. These results highlight the effectiveness of the controller in mitigating harmonics and improving the overall power quality, even under adverse grid conditions and complex load scenarios.

5.3 Simulation result under sag and swell condition

Voltage sag and swell are common power quality disturbances that occur due to sudden changes in load, faults in the power system, or switching operations. Figure 12 illustrates the simulation results under sag and swell conditions, considering a solar irradiance of 1000 W/m². The figure comprises nine waveforms, including three-phase grid voltage with sag and swell,

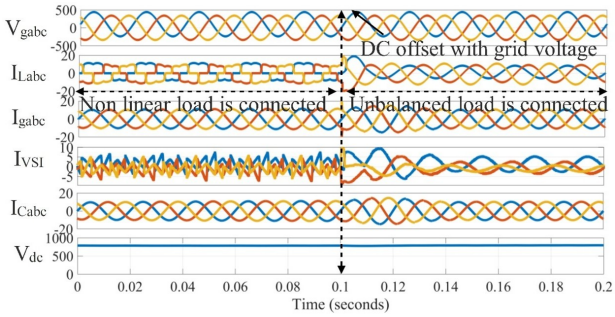

***Fig. 9**: Simulation under grid voltage with DC offset, nonlinear and unbalanced load condition at a solar irradiance of 0 W/m^2.*

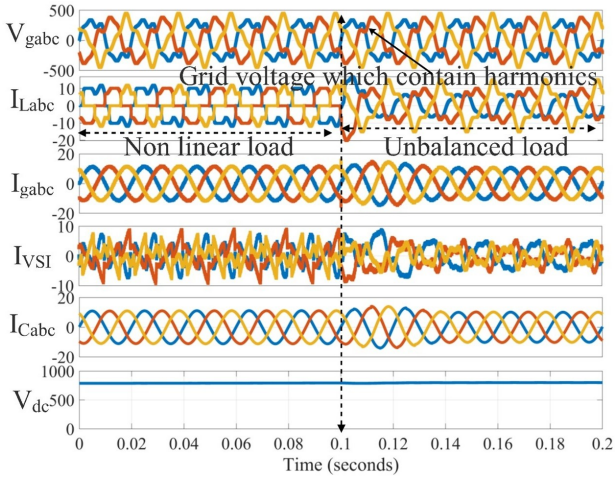

***Fig. 10**: Simulation under grid voltage with harmonics, non-linear and unbalanced load condition at a solar irradiance of 0 W/m^2*

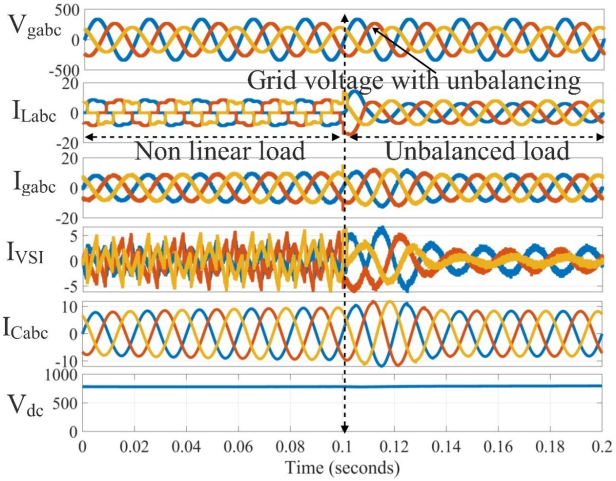

***Fig. 11**: Simulation under unbalanced grid voltage conditions with nonlinear and unbalanced loads at a solar irradiance of 0 W/m^2.*

positive sequence grid current, positive sequence alpha-beta components of the grid current, three-phase load current, negative sequence components of the load

***Table 2**: Comparative THD analysis before and after applying the controller.*

Operating condition	% THD before controller application	% THD after controller application with solar PV	% THD after controller application without solar PV
Normal grid voltage with nonlinear load	28.33 %	0.96 %	3.37 %
Grid voltage with DC offset and nonlinear load	28.46 %	0.93 %	3.22 %
Grid voltage with harmonics and nonlinear load	38.16 %	1.66 %	3.22 %
Unbalanced grid voltage with nonlinear load	25.85 %	0.70 %	4.07 %
Normal grid voltage with unbalanced load	-	0.74 %	3.80 %
Grid voltage with DC offset and unbalanced load	-	0.79 %	3.80 %
Grid voltage with harmonics and unbalanced load	25 %	1.41 %	3.54 %
Unbalanced grid voltage with unbalanced load	-	0.65 %	4.65 %
Sag with nonlinear load	28.33 %	1.45 %	-
Swell with nonlinear load	28.33 %	1.89 %	-

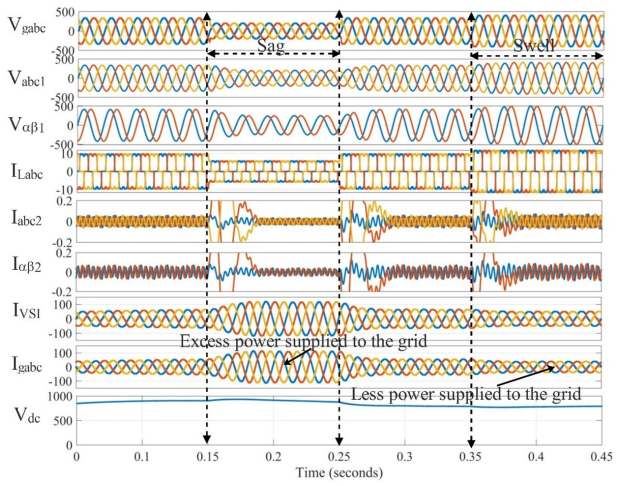

***Fig. 12**: Simulation result under sag and swell condition.*

current, alpha-beta components of the load current, VSI output current, three-phase grid current, and DC link voltage. The simulation was conducted using MATLAB software, where a three-phase programmable source block was employed to generate the sag and swell conditions. The analysis considers a nonlinear load, with the sag condition occurring between 0.15 and 0.25 seconds and the swell condition occurring between 0.35 and 0.45 seconds. During the sag condition, the grid voltage decreases, leading to a reduction in the demand for load current. Consequently, the power generated by the solar PV system is distributed such that less power is supplied to the load, while a greater portion is fed back into the grid, as observed in the eighth waveform of the simulation results. Conversely, during the swell condition, the grid voltage increases, reducing the load current demand. As a result, less power is transferred to the grid, which is also evident in the eighth waveform of the figure. These findings demonstrate the impact of voltage variations on power distribution and highlight the role of solar PV in maintaining system stability under fluctuating grid conditions. Also, the grid current is compositely sinusoidal whose FFT analysis done which is shown in Table 2 which is less than 5%.

5.4 Simulation result under changing solar irradiance condition

Figure 13 presents the simulation results under varying solar irradiance conditions, illustrating the impact on power generation and distribution. The figure includes seven waveforms: solar PV output current, solar PV generated output voltage, solar power generated, load power demand, VSI output power, grid power, and three-phase grid current. As solar irradiance fluctuates, the corresponding solar PV output current also varies, as depicted in the first waveform. From 0 to 0.2 seconds, the solar irradiance decreases; however, the PV system continues to generate sufficient power, which is first

***Table 3**: Comparative analysis of the proposed controller to previously published controller.*

Controller	IRPT [8]	SRF [7]	ADALINE [9]	LMS [11]	Proposed
Controller category	Conventional	Conventional	Adaptive	Adaptive	Adaptive
Oscillation in the output	More	More	More	More	Less
Complexity of the controller	Less	Less	More	More	Less
Extraction of positive sequence component	Not possible	Not possible	Not possible	Not possible	Possible
Grid synchronization	Poor	Good	Poor	Poor	Best
Accuracy	Less	Less	Less	Less	High
DC link voltage	Not stable	Less stable	Not stable	Not stable	More stable
PLL	Not required	Required	Not required	Not required	Not required
DC offset elimination capability	No	No	No	No	Yes
Current harmonics elimination	Less	Less	Less	Less	High
Voltage harmonics elimination	No	No	No	No	Yes
Lower order harmonics elimination	Less	Less	Less	Less	High
Higher harmonics elimination	Less	Less	Less	Less	High
Voltage unbalancing elimination	No	No	No	No	Yes
Current unbalancing elimination	Less	Less	Less	Less	High
Performance of under sag condition	Less	Less	Less	Less	High
Performance of under swell condition	Less	Less	Less	Less	High
Performance under changing solar irradiance	Bad	Normal	Bad	Bad	High
Power factor	Low	Low	Low	Low	High
Sampling time for simulation	5 μs	5 μs	5 μs	5 μs	5 μs

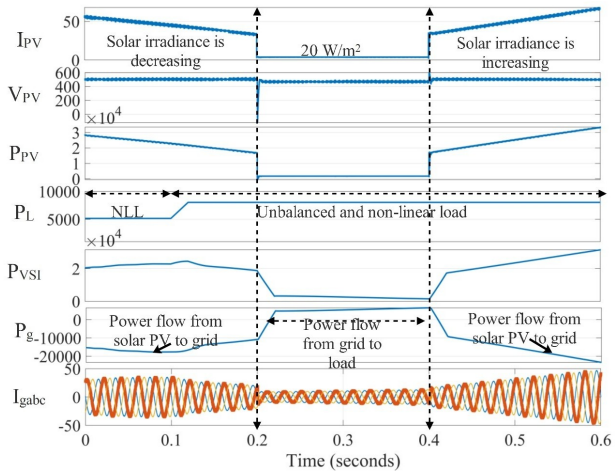

***Fig. 13**: Simulation result under changing solar irradiance condition.*

supplied to the load and then to the grid, indicated by the negative power in the sixth waveform. Between 0.2 and 0.4 seconds, solar irradiance remains constant at a very low level of approximately 20 W/m^2, resulting in minimal or no power generation from the PV system. Under this condition, the grid supplies power to the load, as shown by the positive power in the sixth waveform. From 0.4 to 0.6 seconds, solar irradiance increases again, leading to a rise in solar PV power generation. Consequently, grid power becomes negative once more, indicating that excess power from the PV system is being fed into the grid. Throughout these variations, the three-phase grid current remains purely sinusoidal, demonstrating the effectiveness of the controller in maintaining stable and efficient power flow under dynamic operating conditions.

5.5 Power factor under various grid voltage scenario with non-linear load condition

In grid-connected solar PV systems, low power factor can result from various factors, including the presence of harmonics, voltage imbalances, and DC offsets in the grid voltage, as well as the impact of nonlinear loads. These factors introduce distortions in the current waveform, leading to reduced power factor and inefficient power transfer. Figure 14 illustrates the power factor

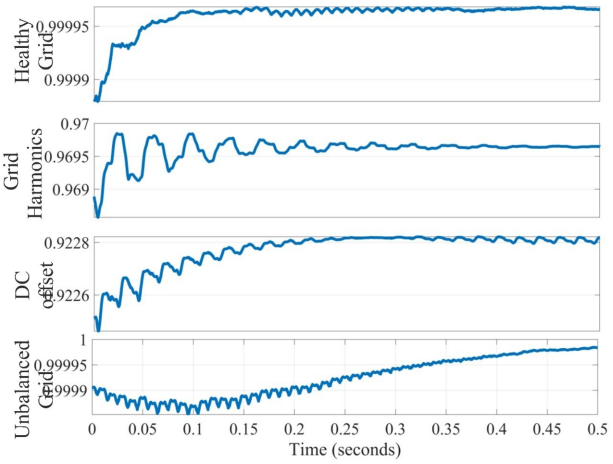

***Fig. 14**: Power factor under various grid voltage scenario with non-linear load condition.*

under different grid voltage scenarios with nonlinear load conditions. The simulation results present four distinct waveforms: power factor under healthy grid voltage conditions, power factor under grid harmonics conditions, power factor under grid voltage with DC offset conditions, and power factor under unbalanced grid voltage conditions. It is evident from the results that, prior to implementing the proposed controller, these grid disturbances significantly affect the power factor. However, after applying the proposed controller, the power factor under all grid voltage conditions is approximately unity. This demonstrates the effectiveness of the proposed controller in mitigating the adverse effects of grid disturbances and maintaining a unity power factor, thereby improving the overall power quality and efficiency of the system.

5.6 FFT analysis

Table 2 presents the FFT analysis of the grid current under various grid voltage and load conditions, both before and after applying the proposed controller. It is observed that before applying the controller, the Total Harmonic Distortion (THD) in the grid current exceeds 5%, whereas after the implementation of the controller, the THD is effectively reduced to below 5% for both cases—with and without solar PV integration. This significant reduction in THD demonstrates the effectiveness of the proposed controller in improving the power quality of the system. Hence, from Table 2, it can be concluded that the proposed controller successfully mitigates various power quality issues under different grid voltage and load conditions.

6. COMPARATIVE ANALYSIS OF THE PROPOSED CONTROLLER TO PREVIOUSLY PUBLISHED CONTROLLER

A detailed comparative evaluation of the proposed adaptive controller against various previously reported conventional and adaptive control techniques is presented in Table 3. The comparison considers several key performance parameters, including control complexity, grid synchronization capability, accuracy, DC-link voltage stability, harmonic elimination, and performance under abnormal grid and solar conditions. The proposed adaptive controller exhibits superior dynamic performance with significantly reduced oscillations in the output, enhanced accuracy, and improved DC-link voltage stability compared to earlier controllers. Unlike other methods, it can extract the positive sequence component and effectively eliminate DC offset, voltage and current harmonics, as well as lower- and higher-order harmonic distortions. Furthermore, it demonstrates excellent performance under grid voltage unbalance, voltage sag and swell, and varying solar irradiance conditions, while maintaining a high-power factor. In contrast, conventional controllers suffer from higher oscillations, poor harmonic compensation, and instability under dynamic grid and load conditions. Earlier adaptive controllers show moderate improvements but still lack effective DC offset removal and harmonic mitigation capabilities. The proposed controller, while maintaining low implementation complexity and similar sampling time (5 μs), achieves best-in-class performance in all critical evaluation metrics, validating its robustness and effectiveness for grid-tied PV systems under diverse operating scenarios.

7. CONCLUSION

This research presents a modified control scheme for grid-connected inverters that enhances the integration of renewable energy sources by effectively addressing challenges posed by unhealthy voltage and current conditions. The proposed improved instantaneous reactive power theory (IIRPT) utilizes positive sequence components from grid voltages and negative sequence elements from load currents to regulate the grid-tied converter. By incorporating a proportional-integral (PI) controller, the scheme effectively manages the DC bus voltage under various grid disturbances and load conditions. The performance of the proposed method is thoroughly evaluated in Matlab/Simulink across multiple operating scenarios, including steady-state, DC offset, grid harmonics, unbalanced grid voltages, and nonlinear and unbalanced loads, both with and without solar PV integration. The results confirm significant improvements in power factor and reactive power compensation, demonstrating the controller's capability to maintain grid stability under varying irradiance levels. Additionally, comparative analysis with existing studies highlights the superiority of the proposed scheme, while the FFT analysis of the grid current verifies that the total harmonic distortion (THD) remains within IEEE-519 standards. These findings validate the robustness and reliability of the proposed control approach, making it a viable solution for enhancing the performance and power quality of grid-connected renewable energy systems.

REFERENCES

[1] G. S. Chawda, A. G. Shaik, M. Shaik, S. Padmanaban, J. B. Holm-Nielsen, O. P. Mahela, P. Kaliannan, "Comprehensive review on detection and classification of power quality disturbances in utility grid with renewable energy penetration," *IEEE Access*, vol. 8, pp. 146807-146830, Aug 2020.

[2] P. Nema, S. V and N. B. P, "Harmonics Mitigation of Grid-Connected Solar PV using Dual Modified Reduced Order Generalized Integrator," *2023 Fourth International Conference on Smart Technologies in Computing, Electrical and Electronics (ICSTCEE)*, Bengaluru, India, 2023, pp. 1-5.

[3] J. A. Eslava Tovar, G. Ramos, D. Celeita and P. Dehghanian, "Harmonic Characterization and Mitigation Strategies for PV-Integrated Distribution Systems: IEEE Std 519-1992 Compliance," *2025 IEEE Workshop on Power Electronics and Power Quality Applications (PEPQA)*, Cartagena, Colombia, 2025, pp. 1-6.

[4] S. Salman, X. Ai, Z. Wu, "Design of a P-&-O algorithm based MPPT charge controller for a stand-alone 200W PV system," *Protection and control of modern power systems*, vol. 3, no. 1, pp. 1-8, Dec 2018.

[5] K.S. Tey, S. Mekhilef, "Modified incremental conductance MPPT algorithm to mitigate inaccurate responses under fast-changing solar irradiation level," *Solar energy*, vol. 101, pp. 333-342, Mar 2014.

[6] P.V. Ramana, K.M. Rosalina, "Optimizing weak grid integrated wind energy systems using ANFIS-SRF controlled DSTATCOM," *Scientific Reports*, vol. 15, no. 1, pp. 13662, Apr 2025.

[7] P.N. Babu, S.K. Bisoyi, D. Sen, S. Pathak, D. Adhikari, P. Nema, G. Panda, "Modified synchronous reference controller for three-phase inverter," In *International Symposium on Sustainable Energy and Technological Advancements*, Singapore: Springer Nature Singapore, 2024, pp. 257-272.

[8] B. Singh, D. T. Shahani and A. K. Verma, "IRPT based control of a 50 kw grid interfaced solar photovoltaic power generating system with power quality improvement," *2013 4th IEEE International Symposium on Power Electronics for Distributed Generation Systems (PEDG)*, Rogers, AR, USA, 2013, pp. 1-8.

[9] P. Nema, V. Sivasankaran, "ADALINE generalized integrator-based control to mitigate the power quality issues in grid connected solar PV systems," *AIP Advances*, vol. 15, no. 2, Feb 2025.

[10] S.R. Das, P.K. Ray, A. Mohanty, "Improvement in power quality using hybrid power filters based on RLS algorithm," *Energy Procedia*, vol. 138, pp. 723-728, Oct 2017.

[11] M. Ahmad, S. Kirmani, "Performance analysis of LMS based control algorithm for power quality improvement in three phase grid connected system for linear/non-linear load," *International Journal of Power Electronics and Drive Systems*, vol. 10, no. 4, pp. 1944. Dec 2019.

[12] R.N. Rao, M. Sreenivasulu, B. Ramakrishna, "Study and analysis of modified LMF control method for power quality improvement," *International Journal of Power Electronics and Drive Systems (IJPEDS)*, vol. 14, no. 2, pp. 992-1000, Jun 2023.

[13] B. Singh, C. Jain, S. Goel, "ILST control algorithm of single-stage dual purpose grid connected solar PV system," *IEEE Transactions on Power Electronics*, vol. 29, no.10, pp. 5347-5357, Dec 2013.

[14] C. Jagadeesh, S.R. Arya, "Variable steps least mean square in wind-based standalone distributed generation system for power quality features," *Electrical Engineering*, vol. 107, no. 7, pp. 8229-8242, Jul 2025.

[15] S.R. Arya, R. Maurya, T.A. Naidu, "Amplitude adaptive notch filter with optimized PI gains for mitigation of voltage-based power quality problems," *CPSS Transactions on Power Electronics and Applications*, vol. 4, pp. 313-23, Dec 2018.

[16] S. K. Singh, S. Ghosh, A. K. Singh and S. N. Singh, "Power Quality Enhancement using Dual-SOGI PLL with Pre-filter based Control Algorithm for DVR in Distorted Grid Conditions," *2025 IEEE International Conference on Computer, Electronics, Electrical Engineering & their Applications (IC2E3)*, Srinagar Garhwal, India, 2025, pp. 1-6.

[17] B. Singh, P. Shah, I. Hussain, "ISOGI-Q based control algorithm for a single stage grid tied SPV system," *IEEE Transactions on Industry Applications*, vol. 54, no.2, pp. 1136-45, Dec 2017.

[18] S. Chakraborty, G. Modi, B. Singh, "MSTOGI-FLL-ROGI based frequency adaptive control for a single stage SPVA-BES-BDC-DG set connected standalone microgrid for remote areas," *IEEE Transactions on Industry Applications*, vol. 59, no. 3, pp. 3727-40, Feb 2023.

[19] G. Modi, B. Singh, "Improved cascaded SOGI control for islanding-synchronization in photovoltaic system", *IEEE Transactions on Industry Applications*, vol. 58, no. 6, pp. 6909-19, Aug 2022.

[20] H. K. Yada and A. S. Kumar, "An SO-SOGI based control for a three-phase DVR under distorted grid conditions including DC offset," *TENCON 2017 - 2017 IEEE Region 10 Conference*, Penang, Malaysia, 2017, pp. 3000-3005.

[21] V. Narayanan, B. Singh," CNISOGI and VSSM-CLMS filters for solving grid and load abnormalities for a microgrid with seamless mode transfer capability," *IEEE Transactions on Industry Applications*, vol. 59, no. 4, pp. 4225-37, Mar 2023.

[22] N. Kumar, I. Hussain, B. Singh, B.K. Panigrahi, "Implementation of multilayer fifth-order generalized integrator-based adaptive control for grid-tied solar PV energy conversion system," *IEEE Transactions on Industrial Informatics*, vol. 14, no. 7, pp. 2857-68, Nov 2017.

[23] P. Nema, V. Sivasankaran, P.N. Babu, "Sixth Order Generalized Integrator Based Power Quality Improvement in Renewable Energy Systems," *Scientia Iranica*, Feb 2025.

Priyank Nema is presently working as an Assistant Professor in the Department of Computer Science and Engineering at Lakshmi Narain College of Technology and Science (LNCTS), Bhopal, India. He has completed his PhD from the School of Electrical and Electronics Engineering at VIT Bhopal University, Sehore, India. His research primarily focuses on addressing power quality issues in grid-connected solar photovoltaic (PV) systems, which is a crucial aspect of the large-scale integration of renewable energy into modern power grids. He received his Bachelor of Engineering (BE) degree in Electrical and Electronics Engineering in 2010 from the University Institute of Technology, Rajiv Gandhi Proudyogiki Vishwavidyalaya (UIT-RGPV), Bhopal, and subsequently earned his Master of Technology (M.Tech) degree in 2012 from the Maulana Azad National Institute of Technology (MANIT), Bhopal, where he strengthened his expertise in electrical engineering and power systems. With a strong academic background and interdisciplinary experience, his research contributions aim to enhance the stability, reliability, and efficiency of grid-connected renewable energy systems, thereby supporting the advancement of sustainable and resilient power networks.

V Sivasankaran is a Senior Assistant Professor in School of Electrical and Electronics Engineering at VIT Bhopal University, Sehore India. And has more than 15 years of teaching and research experience; he completed his B.E with specialization in ECE and M.E with specialization of Applied Electronics and Doctorate in the faculty of Information and Communication Engineering. He obtained All UG, PG and PhD from Anna University Chennai. India. He has published 22 papers in peer reviewed international journals and in IEEE international conferences. He also published book chapters and three patents to his credit. He has is reviewer for various reputed international journal. His research interest is in the areas of control systems, IoT based systems design, Heterogenous wireless networks He had been as session chair for various international conferences across the country also he invited as guest speaker at various seminars and workshops.